Journal of Cerebral Blood Flow & Metabolism (2013) 33, 826–833

www.jcbfm.com

ORIGINAL ARTICLE

# Cerebral blood flow changes after brain injury in human amyloid-beta knock-in mice

Eric E Abrahamson[1,2], Lesley M Foley[3], Steven T DeKosky[4], T Kevin Hitchens[3], Chien Ho[3], Patrick M Kochanek[5,6] and Milos D Ikonomovic[1,2,7]

Traumatic brain injury (TBI) is an environmental risk factor for Alzheimer's disease (AD). Increased brain concentrations of amyloid-$\beta$ (A$\beta$) peptides and impaired cerebral blood flow (CBF) are shared pathologic features of TBI and AD and promising therapeutic targets. We used arterial spin-labeling magnetic resonance imaging to examine if CBF changes after TBI are influenced by human A$\beta$ and amenable to simvastatin therapy. CBF was measured 3 days and 3 weeks after controlled cortical impact (CCI) injury in transgenic human A$\beta$-expressing APP$^{NLh/NLh}$ mice compared to murine A$\beta$-expressing C57Bl/6J wild types. Compared to uninjured littermates, CBF was reduced in the cortex of the injured hemisphere in both A$\beta$ transgenics and wild types; deficits were more pronounced in the transgenic group, which exhibited injury-induced increased concentrations of human A$\beta$. In the hemisphere contralateral to CCI, CBF levels were stable in A$\beta$ transgenic mice but increased in wild-type mice, both relative to uninjured littermates. Post-injury treatment of A$\beta$ transgenic mice with simvastatin lowered brain A$\beta$ concentrations, attenuated deficits in CBF ipsilateral to injury, restored hyperemia contralateral to injury, and reduced brain tissue loss. Future studies examining long-term effects of simvastatin therapy on CBF and chronic neurodegenerative changes after TBI are warranted.

*Journal of Cerebral Blood Flow & Metabolism* (2013) **33,** 826–833; doi:10.1038/jcbfm.2013.24; published online 27 February 2013

**Keywords:** Alzheimer's disease; amyloid; arterial spin-labeling MRI; blood flow; brain injury; statin

## INTRODUCTION

Traumatic brain injury (TBI) is the leading cause of morbidity and mortality in the developed world's working-age population. The burden of severe TBI on the health-care system is exacerbated by increased incidence of Alzheimer's disease (AD) in long-term survivors of TBI[1] and lack of effective therapies for either disorder.

Several neuropathologic parallels link TBI with AD.These include reduced cerebral blood flow (CBF) and increased brain concentrations of amyloid-$\beta$ (A$\beta$) peptide; both are potential therapeutic targets. Deficits in CBF are associated with poorer neurologic outcome after TBI[2] and are posited to contribute to increased risk of developing AD.[3] Accumulation of A$\beta$, the principal component of toxic soluble oligomers and fibrillar aggregates in plaques and cerebral vasculature in AD brains,[4] is observed after human TBI[5–7] and after experimental TBI.[8–12] Brain accumulation of A$\beta$ may be due to injury-induced changes in amyloidogenic (A$\beta$-producing) processing of the amyloid precursor protein (APP), changes in enzymatic degradation of A$\beta$, or alterations in receptors involved in A$\beta$ trafficking and clearance, all of which may be potentiated by brain hypoxia resulting from CBF deficits. The potent vasoactive effects of A$\beta^{13–15}$ may, in turn, result in further reductions in CBF, resulting in a vicious cycle of changes in CBF and A$\beta$ peptide accumulation. These observations, together with the well-characterized pathologic role of A$\beta$ in TBI and AD,[16] warrant identification of therapies with the dual effect of reducing injury or disease-induced pathologic concentrations of A$\beta$ and restoring normal levels of CBF. Ideally, such therapies would have well-characterized beneficial effects on central nervous system structure and function in models of neuronal insult, without harmful side effects.

There are currently no effective treatments for improved recovery and long-term rehabilitation of survivors of TBI, in part owing to lack of clinically relevant experimental models of TBI (particularly those that model TBI-induced increased risk for AD), and the high target specificity of most tested therapies.[17] To directly address these issues, the purpose of this investigation was twofold: (1) to examine the CBF alterations in a preclinical murine model of brain trauma-induced elevations in brain concentrations of human A$\beta$ (APP$^{NLh/NLh}$ human A$\beta$ knock-in mouse model[10]), and (2) to examine the therapeutic effect of the FDA-approved drug, simvastatin, on brain trauma-induced changes in CBF in the same model. Simvastatin was identified as a promising therapeutic candidate because of its beneficial effects in a wide variety of brain injury models (reviewed in Wible and Laskowitz[18]), and more specifically owing to its A$\beta$-reducing and other beneficial effects on histologic and behavioral outcomes after TBI in APP$^{NLh/NLh}$ mice,[10] and its beneficial effects on CBF in A$\beta$ precursor protein (APP)-overexpressing transgenic mouse models of AD.[19,20]

[1]Department of Neurology, University of Pittsburgh, Pittsburgh, Pennsylvania, USA; [2]Geriatric Research Educational and Clinical Center, VA Pittsburgh Healthcare System, Pittsburgh, Pennsylvania, USA; [3]Pittsburgh NMR Center for Biomedical Research, Department of Biological Sciences, Carnegie Mellon University, VA Pittsburgh Healthcare System, Pittsburgh, Pennsylvania, USA; [4]Office of the Dean and Department of Neurology, University of Virginia School of Medicine, Charlottesville, Virginia, USA; [5]Critical Care Medicine, University of Pittsburgh, Pittsburgh, Pennsylvania USA; [6]Safar Center for Resuscitation Research, University of Pittsburgh, Pittsburgh, Pennsylvania, USA and [7]Department of Psychiatry, University of Pittsburgh, Pittsburgh, Pennsylvania, USA. Correspondence: Dr M Ikonomovic, Department of Neurology, University of Pittsburgh, BSTWR S-521, 200 Lothrop Street, Pittsburgh, Pennsylvania 15213, USA.
E-mail: ikonomovicmd@upmc.edu
Supported by NIH P50 NS30318. The Pittsburgh NMR Center for Biomedical Research is supported by a grant from the National Institutes of Health (P41-EB001977). We acknowledge expert technical assistance provided by Mr. William Paljug, Mr. John Melick, and Ms. Lan Shao.
Received 15 August 2012; revised 16 December 2012; accepted 12 January 2013; published online 27 February 2013

## MATERIALS AND METHODS

### Animal Model and Experimental Groups

All experiments were approved by the Animal Care and Use Committees of the University of Pittsburgh and Carnegie Mellon University. Male $APP^{NLh/NLh}$C57Bl/6J ($n = 43$; referred to as $APP^{NLh/NLh}$) and wild-type C57Bl/6J ($n = 23$; Charles River; referred to as C57) mice (aged 100–150 days) were used in these investigations. The $APP^{NLh/NLh}$ mouse has the human Aβ coding sequence 'knocked-in' to the murine APP gene (using site-based mutagenesis), and has the Swedish FADK670N/M671L mutation, which results in production of detectable levels of human Aβ.[21] Unlike traditional APP transgenic mouse models, $APP^{NLh/NLh}$ mice do not overexpress APP, as the APP gene is under the control of its endogenous promoter. Concentrations of human Aβ peptides are amenable to experimental manipulation[9,10] and are detectable by a sensitive human, but not murine, specific enzyme-linked immunosorbent assay.[9,10] Mice were maintained on a 12-hour light–dark cycle with free access to food and water before experimentation. Separate experimental groups included (1) naive (wild-type C57); (2) naive ($APP^{NLh/NLh}$); (3) controlled cortical impact (CCI), 3-day survival (wild-type C57); (4) CCI, 3-day survival ($APP^{NLh/NLh}$), (5) CCI, 3-week survival (wild-type C57); (6) CCI, 3-week survival ($APP^{NLh/NLh}$). The simvastatin intervention experiment was performed on $APP^{NLh/NLh}$ mice only; groups consisted of CCI followed by a 3-week survival with either vehicle or simvastatin treatment.

### Controlled Cortical Impact

Mice were subjected to CCI as described previously.[10] Briefly, anesthesia was induced with 3% isoflurane in $N_2O/O_2$ (1:1; Baxter Pharmaceutical Products, Deerfield, IL, USA) and mice were maintained on 1% to 2% isoflurane for the duration of the surgical procedure (approximately 30 minutes). Mice were placed on a heating pad in a stereotaxic apparatus and an approximately 5-mm-diameter craniotomy was performed over the left parietal–temporal cortex. Body temperature was monitored by a rectal probe (Physitemp Instruments, Clifton, NJ, USA). Mice were subjected to vertically directed CCI (stereotaxic coordinates of the center of the impactor tip relative to Bregma: AP = –2.0; ML = +1.5) using a pneumatic cylinder (Bimba, Monee, IL, USA) with a 3-mm flat-tip impactor at a velocity of 4 m/s, and a depth of 1 mm, using a driving pressure of 73 psi. Immediately after injury, the bone flap was replaced, sealed with Koldmount cement (Vernon Benshoff, Albany, NY, USA), and the scalp closed. Isoflurane was then discontinued and mice were allowed to recover from anesthesia in an oxygen hood for 30 minutes. Mice were then returned to their cages, where they remained under daily observation during the duration of this study.

### Simvastatin Administration

Mice were administered simvastatin (3 mg/kg body weight, determined to be an effective dose in this experimental paradigm[10]) dissolved in 3% methylcellulose by oral gavage starting 3 hours after CCI injury and once daily thereafter for the duration of the experiment (3 weeks).

### Magnetic Resonance Imaging Protocol

Naive mice and injured mice (3 days or 3 weeks after CCI) were intubated and mechanically ventilated with 2% isoflurane and $N_2O/O_2$ (1:1). Physiologic measures, including temperature, blood pressure, and blood gasses, were continuously monitored and adjusted (if necessary) to ensure there were no differences in these variables between groups. A femoral artery catheter was inserted surgically for continuous blood pressure monitoring and arterial blood sampling. Temperature was maintained at $37.0 \pm 0.5^{\circ}C$ using a warm air heating system (SA Instruments, New York, NY, USA). Mean arterial blood pressure and heart rate were also monitored throughout image acquisition. Arterial blood gases were collected at the beginning and end of the studies; ventilator rate and tidal volume were adjusted to maintain an arterial $CO_2$ tension ($PaCO_2$) of 30–45 mm Hg. Mice were considered out of protocol and excluded from the study if the final $PaCO_2$ measurement was outside this range. Mice were placed onto a cradle in the prone position, and the head was secured with ear bars and an adjustable bite bar to limit motion.

MR studies were performed as described previously[22] on a 4.7-T, 40-cm-bore Bruker AVANCE system (Billerica, MA, USA), equipped with a 12-cm-diameter shielded gradient insert and a home-built saddle-type RF coil. Image acquisition parameters were identical to those reported previously.[22] Briefly, $T_2$-weighted images were acquired with the following parameters: field of view 2.5 cm, 1 mm slice thickness, $TR/TE = 2500/40$ milliseconds, two averages, five slices, and a $128 \times 70$ matrix interpolated to $128 \times 128$. Perfusion studies were performed using continuous arterial spin labeling and spin-echo sequence with the following parameters: $64 \times 40$ matrix interpolated to $64 \times 64$, $TR = 2000$ milliseconds, summation of three echoes, $TE = 10$, 20, and 30 milliseconds, and two averages. The labeling pulse for the inversion plane was positioned $\pm 2$ cm from the perfusion detection plane. Spin-labeling efficiency was determined from intensities within the carotid arteries using a gradient echo sequence, with a $45^{\circ}$ flip angle, eight averages, $TR/TE = 100/9.6$ milliseconds, $256 \times 256$ matrix, and spin labeling applied at $\pm 6$ mm. The spin-lattice relaxation time of tissue water ($T_{1obs}$) was measured from a series of spin-echo images with variable TR values of 8,000, 4,300, 2,300, 1,200, 650, 350, 185, and 100 milliseconds.

### Cerebral Blood Flow Image Analysis

Regions of interest (ROIs) included the left (ipsilateral to injury) and right (contralateral to injury) hemispheres and the cortex, cortical contusion region (CR), hippocampus, thalamus, and the amygdala/piriform cortex within each hemisphere in the coronal plane approximately 2 mm caudal to Bregma[23] (Figure 1). Cortical ROIs were drawn to include the entire cortex within each hemisphere (cortex), or an area beginning 1 mm from midline to the midpoint of the arc of the cortex (cortical contusion region; Figure 1). Pixel by pixel maps of $(M_C–M_L)M_C^{-1}$ were generated from the perfusion data, where $M_C$ is the signal intensity from the control image and $M_L$ is the signal intensity from the labeling image. $T_{1obs}$ maps were generated from the series of variable TR images. Regional CBF was then calculated from:

$$CBF = \lambda(T_{1obs} \cdot 2\alpha)^{-1}(M_C - M_L)M_C^{-1} \quad (1)$$

where $\lambda$ is the blood–brain partition coefficient of water, assuming a spatially constant value of 0.9 mL/g, and $\alpha$ is the spin-labeling efficiency measured in the arteries. ROIs were segmented from each CBF map and histograms were generated for each time point and genotype.

### *Ex Vivo* Magnetic Resonance Image Acquisition

After *in vivo* MRI evaluation, the mice were perfused and brains processed using the histologic analysis protocol described below. The fixed brains were imaged using an 11.7-T, 89-mm-bore Bruker AVANCE spectrometer, equipped with a Micro 2.5 gradient insert. High-resolution 3D images were acquired with the following parameters: $TR = 500$ milliseconds, $TE = 6$ milliseconds, $FOV = 1 \times 1 \times 1.7\ cm^3$, four averages, with an approximate isotropic resolution of 40 μm. Lesion size was assessed in eight planes through the brain lesion. Percent tissue loss was determined for the whole hemisphere, as the anatomic resolution of the MRI precluded accurate measurements of the hippocampus.

### Histologic Assessment of Brain Lesion Size

For histologic analyses, mice were anesthetized with 5% isoflurane in $O_2/NO_2$ (1:1) and transcardially perfused with 0.1 mol/L phosphate-buffered saline (pH 7.4). Brains were extracted and fixed for 48 hours in 4% paraformaldehyde made in phosphate-buffered saline (pH 7.4). Cortical lesion volume was determined by calculating the percent tissue loss ipsilateral to injury (compared with the non-injured contralateral cortex) on three Nissl-stained tissue sections through the lesion at the level of the dorsal hippocampus, approximately 1.3, 2.3, and 3.3 μm caudal to Bregma. Using NIH Image (http://rsb.info.nih.gov/nih-image/), the ipsilateral and contralateral cortex and hippocampus were outlined separately to calculate percent tissue area ipsilateral compared with contralateral.

### Aβ ELISA

For biochemical assays of brain Aβ content, mice were anesthetized and transcardially perfused with phosphate-buffered saline. The brain was extracted and immediately dissected on ice, and the hippocampus and cortex ipsilateral and contralateral to injury were isolated, snap frozen in liquid nitrogen, and stored at –80°C until assayed. Frozen brain tissues were sonicated on ice in 0.2% diethylamine and 150 mmol/L NaCl with a protease inhibitor cocktail consisting of 1 mmol/L AEBSF, 0.8 μmol/L aprotinin, 20 μmol/L leupeptin, 40 μmol/L bestatin, 15 μmol/L pepstatin A, and 14 μmol/L E-64, and centrifuged at 135 000 *g* for 1 hour. Levels of human Aβ1-40 and Aβ1-42 were assayed in diethylamine-soluble supernatant, using TMB-based enzyme-linked immunosorbent assay (Invitrogen) as described previously.[9] Aβ values are expressed as femtomoles Aβ per gram tissue wet weight.

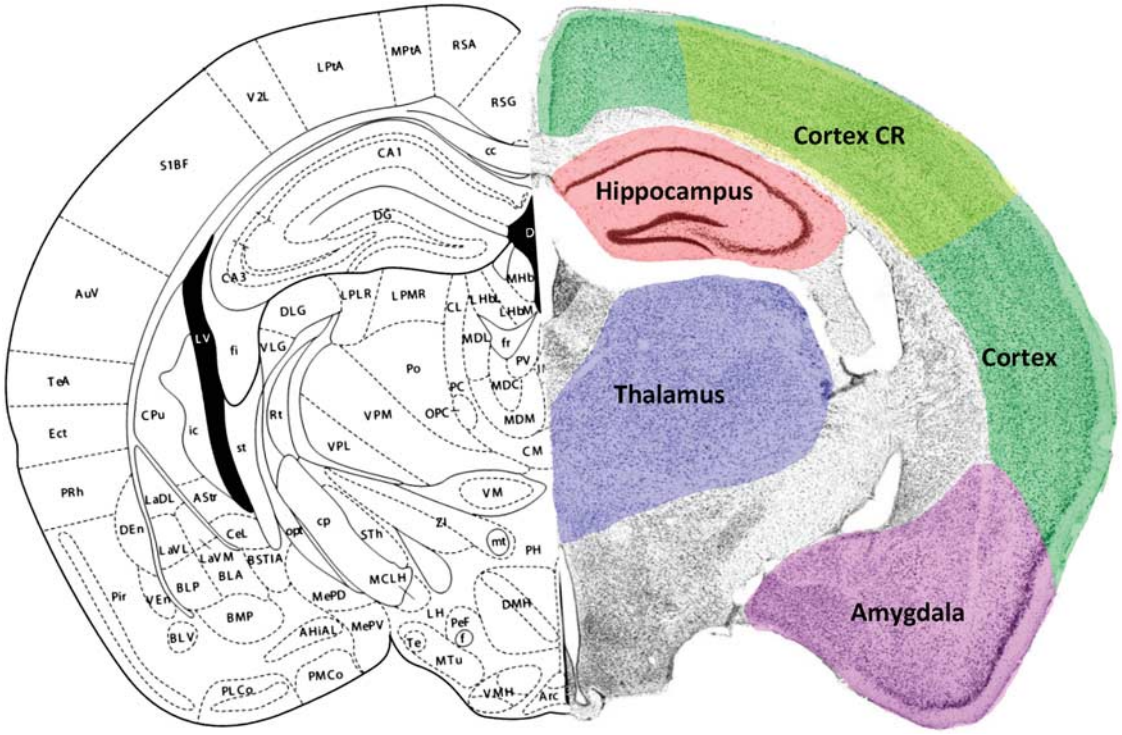


**Figure 1.** Coronal brain section through the dorsal hippocampus illustrating regions of interest (ROIs) examined in this study. Left hemisphere taken from Franklin and Paxinos[23] at approximately 2.0 mm caudal to Bregma. Right hemisphere illustrates a cresyl violet-processed section with ROI outlined in color. The color reproduction of this figure is available on the *JCBFM* journal online. CR, contusion region.

**Table 1.** Physiologic data[a]

| | *WT naive* (n = *4*) | *hAβ naive* (n = *4*) | *WT 3 days after CCI* (n = *5*) | *hAβ 3 days after CCI* (n = *5*) | *WT 3 weeks after CCI* (n = *6*) | *hAβ 3 weeks after CCI* (n = *6*) | *hAβ 3 weeks after CCI/veh* (n = *10*) | *hAβ 3 weeks after CCI/simva* (n = *9*) |
|---|---|---|---|---|---|---|---|---|
| pH | 7.42 ± 0.02 | 7.4 ± 0.03 | 7.38 ± 0.04 | 7.41 ± 0.03 | 7.44 ± 0.03 | 7.41 ± 0.02 | 7.39 ± 0.03 | 7.4 ± 0.05 |
| $PaCO_2$ | 36.4 ± 2.1 | 35.1 ± 1.8 | 36.1 ± 3 | 36.6 ± 2.1 | 35.6 ± 2.6 | 36.5 ± 4.3 | 37.8 ± 3.85 | 35.6 ± 6.0 |
| $PaO_2$ | 240 ± 12 | 243 ± 8.6 | 244 ± 15.1 | 240 ± 11 | 238.5 ± 9.3 | 245 ± 8.2 | 240.5 ± 9.3 | 231.6 ± 34.2 |
| MABP | 82 ± 11.6 | 89.1 ± 9 | 91.1 ± 13.6 | 77 ± 10 | 81.8 ± 15.1 | 79 ± 12.6 | 86 ± 9 | 83 ± 10.3 |
| Heart rate | 485 ± 65 | 502 ± 112 | 499 ± 83 | 475 ± 75 | 519 ± 92 | 496 ± 55 | 475 ± 121 | 504 ± 94 |
| Weight (g) | 28 ± 2 | 31 ± 1.4 | 31 ± 0.9 | 28 ± 1 | 31 ± 2.1 | 33 ± 1.3 | 29 ± 1.2 | 30 ± 0.6 |

Abbreviations: CCI, controlled cortical impact; MABP, mean arterial blood pressure; veh, vehicle; WT, wild type. Data were collected before and after perfusion imaging and averaged. All variables were within normal range.
[a]Data are mean ± SD.

### Statistical Analysis

All data are expressed as mean ± standard deviation. Independent C57 and $APP^{NLh/NLh}$ mice were studied for each time point (naive, 3 days, and 3 weeks). Data from C57 and $APP^{NLh/NLh}$ were compared at each time point using a two-tailed Student's *t*-test. A probability of less than 0.05 ($P < 0.05$) was considered significant.

## RESULTS

### Physiology Parameters and Baseline Regional CBF

There were no differences in arterial blood gasses, hematocrit, blood glucose, blood pH, or mean arterial blood pressure between groups of injured and uninjured (naive) C57 or $APP^{NLh/NLh}$ mice, and injured $APP^{NLh/NLh}$ mice administered simvastatin or vehicle (Table 1).

In naive C57 and $APP^{NLh/NLh}$ mice, CBF values were comparable in the brain regions examined (Figures 2 and 3). In both C57 and $APP^{NLh/NLh}$ mice, CBF was highest in the thalamus (251.5 ± 23.3 and 251.5 ± 45.6 mL per 100 g per minute, respectively) and lowest in the amygdala (157.0 ± 23.9 and 164.7 ± 34.5 mL per 100 g per minute, respectively).

### Regional CBF Changes 3 Days and 3 Weeks After CCI Injury

*CBF ipsilateral to injury (3 days).* Compared to the naive groups, CBF values in injured C57 and $APP^{NLh/NLh}$ mice were similarly reduced in the cortex and the cortical CR ipsilateral to injury ($P < 0.05$ compared with naive). CBF values in the thalamus of the injured C57 group were higher than in the C57 naive group ($P < 0.05$). CBF in the thalamus of the injured $APP^{NLh/NLh}$ group was not significantly different from the $APP^{NLh/NLh}$ naive group, but was lower than in the injured C57 group ($P < 0.05$; Figures 2 and 3).

*CBF contralateral to injury (3days).* The injured C57 group had higher CBF values in the hemisphere and thalamus ($P < 0.05$),

and in the amygdala, cortex, and in the cortical CR (corresponding to the contusion region on the side of the injury; $P<0.01$), compared to naive C57 controls. CBF in the hemisphere and thalamus of the injured $APP^{NLh/NLh}$ group was lower than in the injured C57 group ($P<0.05$; Figures 2 and 3) and did not differ the naive $APP^{NLh/NLh}$ group.

*CBF ipsilateral to injury (3 weeks)*. Compared to naive groups, injured C57 and $APP^{NLh/NLh}$ groups had lower CBF values in the cortex and cortical CR ($P<0.05$, with the exception of the C57 cortex, which did not reach statistical significance). The injured $APP^{NLh/NLh}$ group had lower CBF values in the cortex and thalamus

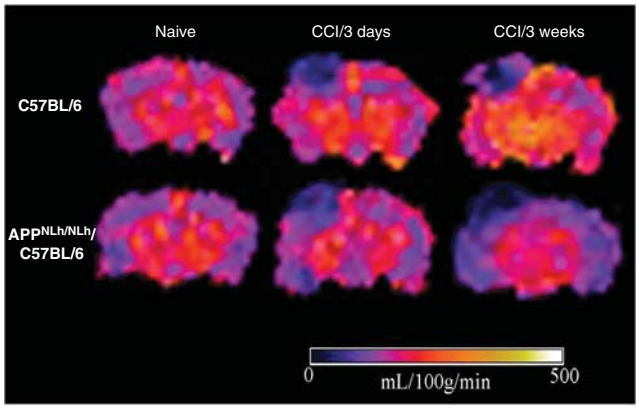


**Figure 2.** Representative cerebral blood flow (CBF) maps illustrated on coronal views of arterial spin-labeling MR images taken at the level of the dorsal hippocampus from naive and injured C57 and $APP^{NLh/NLh}$ mice. CBF levels in each region of interest defined in Materials and Methods were quantified and are illustrated in Figure 3. CCI, controlled cortical impact.

($P<0.05$) and in the hemisphere and cortical CR ($P<0.01$) when compared with the injured C57 group (Figure 3).

*CBF contralateral to injury (3 weeks)*. The injured C57 group had higher CBF values in the amygdala ($P<0.05$), and in the hemisphere, thalamus, cortex, and the cortical CR ($P<0.01$) when compared with naive groups. CBF values in the injured $APP^{NLh/NLh}$ group were lower in the cortex and cortex CR ($P<0.05$) and in the hemisphere and amygdala ($P<0.01$) compared with the injured C57 group (Figure 3) and did not differ in any region compared with the $APP^{NLh/NLh}$ naïve group.

*Effect of simvastatin therapy on CBF after CCI injury in $APP^{NLh/NLh}$ mice (3 weeks)*. We next examined the effects of postinjury treatment with simvastatin (3 mg/kg daily by oral gavage) or vehicle on CBF in $APP^{NLh/NLh}$ mice 3 weeks after CCI injury. Compared with vehicle-treated $APP^{NLh/NLh}$ mice, simvastatin-treated $APP^{NLh/NLh}$ mice had significantly higher CBF values bilaterally in the thalamus and in the contralateral cortical CR region compared with vehicle-treated $APP^{NLh/NLh}$ mice ($P<0.05$; Figure 4). There was a trend for higher CBF in the ipsilateral hippocampus and the contralateral cortex and amygdala in the simvastatin group compared with the vehicle group (Figure 4).

*Effects of simvastatin therapy after CCI: relation to lesion volume and brain Aβ concentration in $APP^{NLh/NLh}$ mice (3 weeks)*. By *ex vivo* MR imaging, $APP^{NLh/NLh}$ mice treated with simvastatin had significantly greater brain tissue sparing compared with vehicle-treated $APP^{NLh/NLh}$ mice ($P<0.05$; Figures 5A and 5B). These observations were confirmed by histologic examination of tissue sections of the same brains (Figures 5C and 5D), although the simvastatin-treatment-associated increase in tissue sparing did not reach statistical significance.

Diethylamine-soluble Aβ peptides were not detectable in C57 mice, and were detected in all $APP^{NLh/NLh}$ brain samples; Aβ1-40

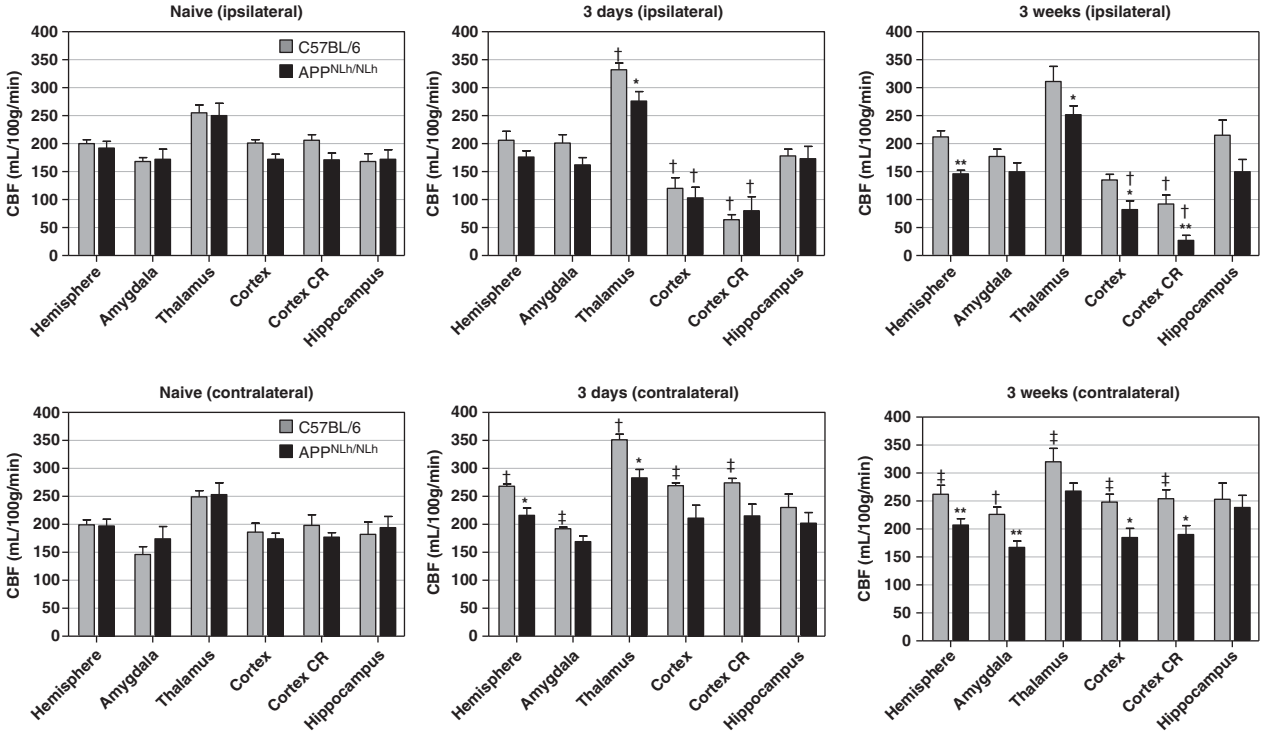


**Figure 3.** Cerebral blood flow (CBF) values in regions of interest in naive and controlled cortical impact injured C57 and $APP^{NLh/NLh}$ mice (mean ± SE). *$APP^{NLh/NLh}$ < C57, $P<0.05$; **$APP^{NLh/NLh}$ < C57, $P<0.01$; †3 days, 3 weeks > naive, $P<0.05$; ‡3 days, 3 weeks compared with naive, $P<0.01$. CR, contusion region.

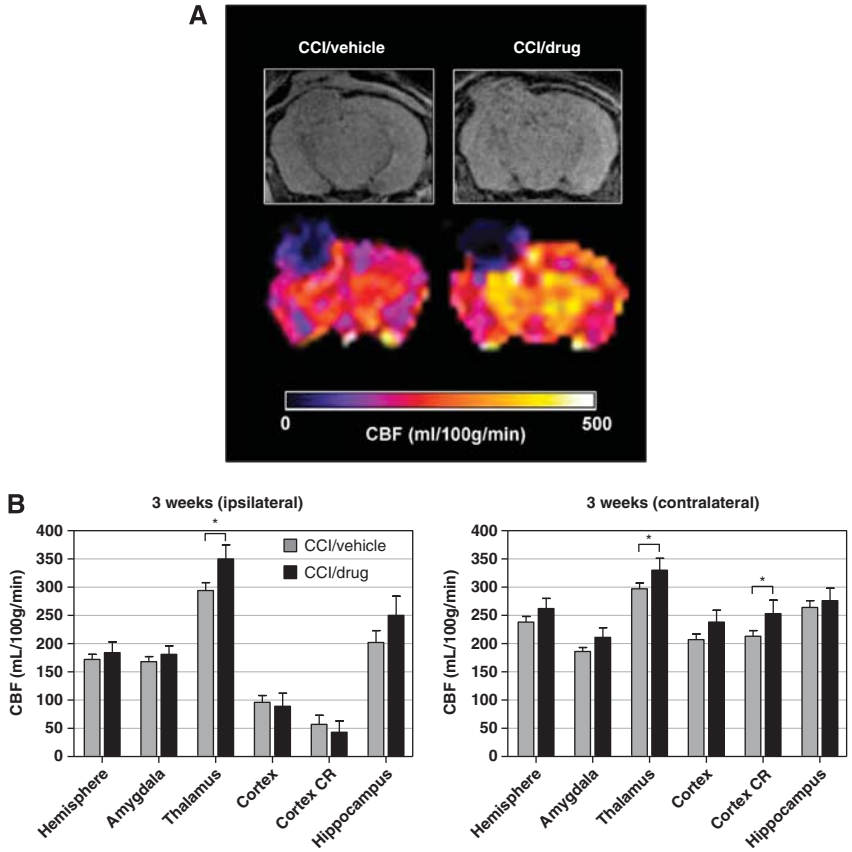


**Figure 4.** (**A**) Representative magnetic resonance image (**A**, top row) cerebral blood flow (CBF; **A**, bottom row) maps illustrated in coronal views at the level of the dorsal hippocampus from $APP^{NLh/NLh}$ mice after controlled cortical impact (CCI) injury and 3 weeks treatment with either vehicle or 3 mg/kg simvastatin. (**B**) Region of interest CBF values from the two experimental groups with CCI/vehicle (gray bars) and CCI/drug (black bars) treatment. *CCI/drug > CCI/vehicle, $P < 0.05$. CR, contusion region.

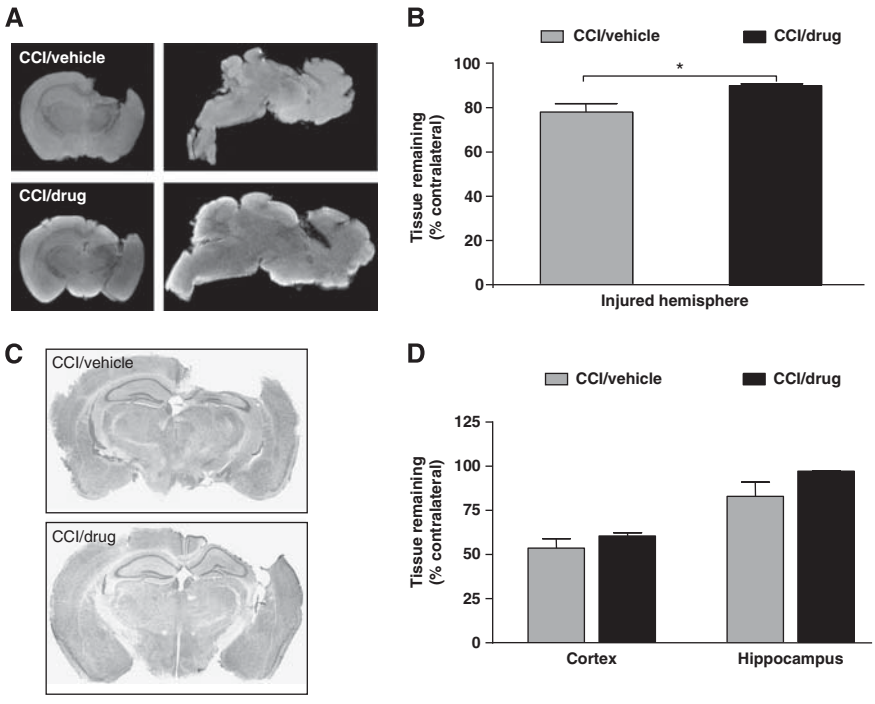


**Figure 5.** Analyses of brain tissue volume in representative magnetic resonance image (MRI) scans *ex vivo* (MRI images, **A**; quantification, **B**) and corresponding histologic sections (photomicrographs, **C**; quantification, **D**) from $APP^{NLh/NLh}$ subjected to controlled cortical impact (CCI) injury and treatment with either vehicle or 3 mg/kg simvastatin for 3 weeks. MRI analysis demonstrates greater tissue preservation in the CCI/drug group. *$P < 0.05$.

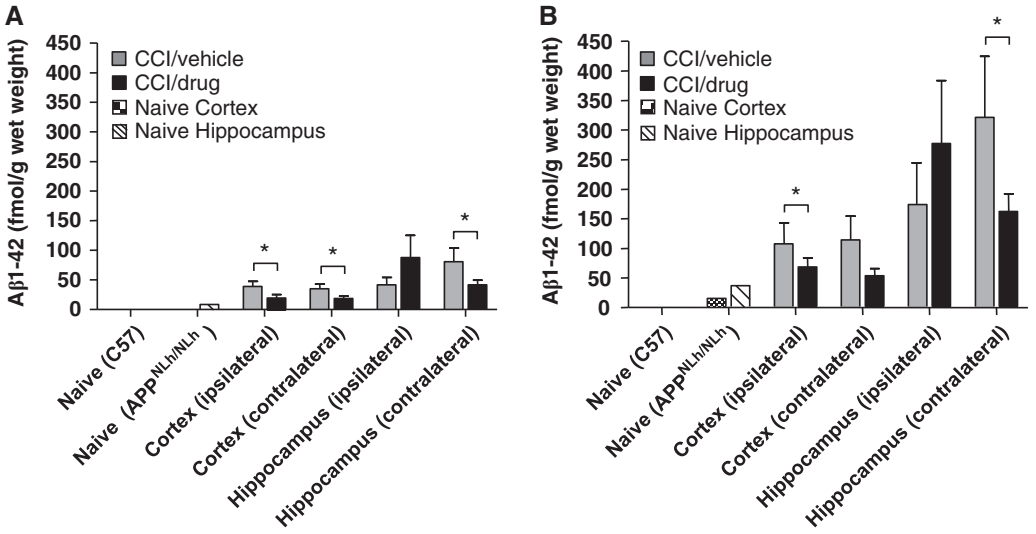


**Figure 6.** Enzyme-linked immunosorbent assay analyses of Aβ1-42 (**A**) and Aβ1-40 (**B**) concentrations in the cortex and hippocampus tissue homogenates from C57 and $APP^{NLh/NLh}$ mice with no injury (naive) or 3 weeks after controlled cortical impact (CCI) injury and administration of either vehicle or 3 mg/kg simvastatin in $APP^{NLh/NLh}$ mice. $^*P < 0.05$.

was consistently higher than Aβ1-42. CCI injury resulted in increases in both Aβ species in the hippocampus and cortex ipsilateral and contralateral to injury relative to the naive group (Figure 6). Injured, simvastatin-treated $APP^{NLh/NLh}$ mice had lower hippocampal and cortical Aβ levels bilaterally compared with injured, vehicle-treated $APP^{NLh/NLh}$ mice ($P < 0.05$) except for the ipsilateral hippocampus (Figure 6). Significantly lower Aβ levels correlated with higher CBF in the contralateral cortex and cortex CR; however, this relationship was not observed in the ipsilateral cortex and cortex CR, where CBF levels remained unchanged relative to vehicle-treated mice despite significant regional reductions in Aβ levels. There was no relationship between Aβ concentrations and CBF levels bilaterally in the hippocampus. There were no differences in Aβ42/40 ratios between groups (not shown). Over all measured regions, there was a trend for an inverse relation between Aβ concentration (summed Aβ40 and Aβ42) and CBF in the contralateral cortex ($r = -0.63$; $P_2 = 0.092$).

## DISCUSSION

The present study demonstrates regional differences in CBF after CCI injury modified by genetic introduction of human Aβ peptides ($APP^{NLh/NLh}$ mice) and simvastatin therapy. Brain injury-induced reductions in CBF were observed in the ipsilateral cerebral cortex and cortical CR of wild-type C57 mice, and were exacerbated in $APP^{NLh/NLh}$ (human Aβ-producing) mice, particularly at longer time points (3 weeks) after injury. In contrast, brain regions contralateral to injury exhibited increased CBF in injured, wild-type C57 mice, with regional and temporal patterns similar but opposite of what was observed in the ipsilateral cortex and cortical CR; these contralateral increases in CBF were blunted in injured $APP^{NLh/NLh}$ mice.

Regional variation in CBF alterations after CCI injury may be the result of different injury and reparative processes in areas subjected to direct mechanical injury and necrotic cell death (e.g., cortex including the contusion region) compared with the hippocampus and thalamus (and the hemisphere contralateral to CCI injury), which are characterized by secondary injury processes such as glial activation, production of cytokines and reactive oxygen species, and apoptosis, which may result in, or be enhanced in, areas of increased energy utilization.[24] Alternatively, increased CBF in the contralateral hemisphere may result from compensatory or disinhibition processes occurring in response to disrupted neural connectivity. Postinjury hyperemia is observed in humans, particularly in areas of brain tissue without overt damage.[25] Hyperemia is attenuated in aged animals,[26] and may be a necessary condition for recovery from TBI.[2] However, whether CCI injury-induced hyperemia represents CBF dysregulation or a beneficial reactive response to CCI injury in the current model is unknown.

Exacerbated CBF deficits and blunted hyperemia responses after CCI in $APP^{NLh/NLh}$ compared with C57 mice may be due to the observed increases in concentrations of human Aβ, a neurotoxic peptide with potent vasoactive properties. $APP^{NLh/NLh}$ mice exhibited blunted increases in CBF in brain regions contralateral to CCI injury compared with C57 wild types, reminiscent of Aβ-associated attenuation of functional hyperemia in mouse neocortex.[27] Soluble human Aβ may act as a potent vasoconstrictor and modulator of CBF through enhancement of endothelin-1 vasoconstriction, stimulation of proinflammatory pathways involving 5-lipoxygenase and cyclooxygenase-2, release of free radicals (reviewed in Iadecola[3] and Townsend *et al*[28]), and impairment of angiogenesis.[29] In transgenic AD mice overexpressing mutant human Aβ-precursor protein (APP), decreases in CBF and impairment of cerebrovascular autoregulation are proportional to brain Aβ levels.[30] These observations suggest that therapeutics, such as simvastatin, that lower Aβ in conditions of brain injury and have complementary CBF-modifying effects have promising clinical potential regardless of the connection between Aβ and CBF, which is likely complex and not amenable to dissection and resolution in *in vivo* models of TBI.

We observed modulatory effects of simvastatin administration on CCI injury-induced changes in CBF and Aβ levels in CCI-injured $APP^{NLh/NLh}$ mice; attenuated deficits in CBF were observed in brain regions ipsilateral to injury and restored hyperemia was observed in brain regions contralateral to injury. CBF-modifying effects of simvastatin treatment after TBI and in other models of impaired CBF were observed previously[19,20,31] and are likely due to the drug's pleiotropic mechanisms of action, including upregulation of endothelial nitric oxide synthase (NOS) with subsequent elevations in NO,[32,33] and reduced production of isoprenoid intermediates in the cholesterol synthesis pathway (reviewed in Laufs and Liao[34]). Simvastatin administration was also reported to associate with 'augmented angiogenesis' after experimental TBI, particularly in the lesion boundary zone,[35] though the role of

angiogenesis in mediating the effects of simvastatin on CBF in the current model is less clear, especially in brain areas distal to the area of mechanical lesion (i.e., lesion boundary zone). Hamel and colleagues[19,20] reported restorative effects of simvastatin on CBF responses to neuronal activation in an uninjured, APP-overexpressing mouse AD model, with parallel reductions in oxidative stress, inflammation, and monomeric Aβ. Simvastatin therapy is also associated with reductions in inflammatory markers in several brain injury models,[36] including the model used in the current experiment;[10] these studies report reductions in activated microglia, particularly relevant to current hypotheses linking TBI, microglia activation, and increased Aβ production (reviewed in Mannix and Whalen[37]). The current report extends these studies by demonstrating that the restorative effects of simvastatin therapy on CBF after TBI occur in parallel with reductions in physiologically soluble Aβ monomers and oligomers in a clinically relevant model of mice expressing human Aβ. Consistent with our previous report,[10] CCI injury in $APP^{NLh/NLh}$ mice resulted in sustained elevations in human Aβ peptides bilaterally in the hippocampus and cortex, which, with the exception of the ipsilateral hippocampus, were suppressed by simvastatin treatment. The mechanisms connecting simvastatin treatment and changes in brain Aβ concentration are likely a combination of direct effects on Aβ production, degradation, or clearance and other, indirect, pathways including reduced microglia activation.[10] CBF was significantly increased in the contralateral cortical CR concomitant with reduced Aβ levels. However, we observed only a weak inverse correlation between Aβ concentrations and CBF levels exclusively in the contralateral cortex. Lack of correlation between these variables could be reflective of a complex relationship between biochemical and *in vivo* imaging measures or other, non-Aβ-related injury responses superimposed on the known vasoactive effects of Aβ. Alternatively, Aβ oligomers may correlate more closely with CBF changes; this may be masked by our enzyme-linked immunosorbent assay protocol, which does not distinguish between Aβ monomers and oligomers. This may also explain the large variability in hippocampal Aβ concentrations, which were not affected by simvastatin ipsilateral to injury. Although this investigation does not prove, nor was it designed to prove, a direct relationship between simvastatin-induced reductions in brain Aβ and associated positive effects on CBF and histologic outcome, the results of this investigation and the previously discussed preclinical reports provide strong rationale for using simvastatin in clinical TBI therapy trials. Furthermore, the nearly unparalleled success of simvastatin in preclinical intervention trials in multiple types of neurologic insult, its safety and tolerance in humans (established over $>20$ years of use in humans), and studies indicating its therapeutic potential in the treatment of human neurologic disorders overwhelmingly support the therapeutic potential of simvastatin.

## DISCLOSURE/CONFLICT OF INTEREST

The authors declare no conflict of interest.

## REFERENCES

1 Van Den Heuvel C, Thornton E, Vink R. Traumatic brain injury and Alzheimer's disease: a review. *Prog Brain Res* 2007; **161**: 303–316.
2 Kelly DF, Martin NA, Kordestani R, Counelis G, Hovda DA, Bergsneider M *et al.* Cerebral blood flow as a predictor of outcome following traumatic brain injury. *J Neurosurg* 1997; **86**: 633–641.
3 Iadecola C. Cerebrovascular effects of amyloid-beta peptides: mechanisms and implications for Alzheimer's dementia. *Cell Mol Neurobiol* 2003; **23**: 681–689.
4 Hardy J, Selkoe DJ. The amyloid hypothesis of Alzheimer's disease: progress and problems on the road to therapeutics. *Science* 2002; **297**: 353–356.
5 Roberts GW, Gentleman SM, Lynch A, Murray L, Landon M, Graham DI. B amyloid protein deposition in the brain after severe head injury: implications for the pathogenesis of Alzheimer's disease. *J Neurol Neurosurg Psych* 1994; **57**: 419–425.
6 Ikonomovic MD, Uryu K, Abrahamson EE, Ciallella JR, Trojanowski JQ, VM-Y Lee *et al.* Alzheimer's pathology in human temporal cortex surgically excised after severe brain injury. *Exp Neurol* 2004; **190**: 192–203.
7 DeKosky ST, Abrahamson EE, Ciallella JR, Paljug WR, Wisniewski SR, Clark RSB *et al.* Association of increased cortical soluble abeta42 levels with diffuse plaques after severe brain injury in humans. *Arch Neurol* 2007; **64**: 541–544.
8 Smith DH, Nakamura M, McIntosh TK, Wang J, Rodriguez A, Chen X-H *et al.* Brain trauma induces massive hippocampal neuron death linked to a surge in beta-amyloid levels in mice overexpressing mutant amyloid precursor protein. *Am J Pathol* 1998; **153**: 1005–1010.
9 Abrahamson EE, Ikonomovic MD, Ciallella JR, Hope CE, Paljug WR, Isanski BA *et al.* Caspase inhibition therapy abolishes brain trauma-induced increases in Abeta peptide: Implications for clinical outcome. *Exp Neurol* 2006; **197**: 437–450.
10 Abrahamson EE, Ikonomovic MD, Dixon CE, DeKosky ST. Simvastatin therapy prevents brain trauma-induced elevations in β-amyloid peptide levels. *Ann Neurol* 2009; **66**: 407–414.
11 Loane DJ, Pocivavsek A, Moussa CE, Thompson R, Matsuoka Y, Faden AI *et al.* Amyloid precursor protein secretases as therapeutic targets for traumatic brain injury. *Nat Med* 2009; **15**: 377–379.
12 Loane D, Washington P, Vardanian L, Pocivavsek A, Hoe HS, Duff KE *et al.* Modulation of ABCA1 by an LXR agonist reduces β-amyloid levels and improves outcome after traumatic brain injury. *J Neurotrauma* 2011; **28**: 225–236.
13 Crawford F, Suo Z, Fang C, Mullan M. Characteristics of the *in vitro* vasoactivity of beta-amyloid peptides. *Exp Neurol* 1998; **150**: 159–168.
14 Suo Z, Humphrey J, Kundtz A, Sethi F, Placzek A, Crawford F *et al.* Soluble Alzheimers beta-amyloid constricts the cerebral vasculature *in vivo*. *Neurosci Lett* 1998; **257**: 77–80.
15 Dietrich HH, Xiang C, Han BH, Zipfel GJ, Holtzman DM. Soluble amyloid-beta, effect on cerebral arteriolar regulation and vascular cells. *Mol Neurodegen* 2010; **5**: 15.
16 DeKosky ST, Ikonomovic MD, Gandy S. Traumatic brain injury: football, warfare, and long-term effects. *N Engl J Med.* 2010; **363**: 1293–1296.
17 Jain KK. Neuroprotection in traumatic brain injury. *Drug Discov Today* 2008; **13**: 1082–1089.
18 Wible EF, Laskowitz DT. Statins in traumatic brain injury. *Neurotherapeutics* 2010; **7**: 62–73.
19 Tong XK, Nicolakakis N, Fernandes P, Ongali B, Brouillette J, Quirion R *et al.* Simvastatin improves cerebrovascular function and counters soluble amyloid-beta, inflammation and oxidative stress in aged APP mice. *Neurobiol Dis* 2009; **35**: 406–414.
20 Tong XK, Lecrux C, Rosa-Neto P, Hamel E. Age-dependent rescue by simvastatin of Alzheimer's disease cerebrovascular and memory deficits. *J Neurosci* 2012; **32**: 4705–4715.
21 Reaume AG, Howland DS, Trusko SP, Savage MJ, Lang DM, Greenberg BD *et al.* Enhanced amyloidogenic processing of the β-amyloid precursor protein in gene-targeted mice bearing the Swedish familial Alzheimer's disease mutations and a "humanized" Aβ sequence. *J Biol Chem* 1996; **271**: 23380–23388.
22 Foley LM, Hitchens TK, Melick JA, Bayir H, Ho C, Kochanek PM. Effect of inducible nitric oxide synthase on cerebral blood flow after experimental traumatic brain injury in mice. *J Neurotrauma* 2008; **25**: 299–310.
23 Franklin KBJ, Paxinos G (eds). *The mouse brain in stereotaxic coordinates*. Academic Press: San Diego, CA, 1997.
24 Tsujimoto Y. Apoptosis and necrosis: intracellular ATP level as a determinant for cell death modes. *Cell Death Differ* 1997; **4**: 429–434.
25 Bullock R, Sakas D, Patterson J, Wyper D, Hadley D, Maxwell W *et al.* Early post-traumatic cerebral blood flow mapping: correlation with structural damage after focal injury. *Acta Neurochir Suppl* 1992; **55**: 14–17.
26 Biagas KV, Grundl PD, Kochanek PM, Schiding JK, Nemoto EM. Posttraumatic hyperemia in immature, mature, and aged rats: autoradiographic determination of cerebral blood flow. *J Neurotrauma* 1996; **13**: 189–200.
27 Park L, Anrather J, Forster C, Kazama K, Carlson GA, Iadecola C. Abeta-induced vascular oxidative stress and attenuation of functional hyperemia in mouse somatosensory cortex. *J Cereb Blood Flow Metab* 2004; **24**: 334–342.
28 Townsend KP, Obregon D, Quadros A, Patel N, Volmar C, Paris D *et al.* Proinflammatory and vasoactive effects of Abeta in the cerebrovasculature. *Ann N Y Acad Sci* 2002; **977**: 65–76.
29 Paris D, Patel N, DelleDonne A, Quadros A, Smeed R, Mullan M. Impaired angiogenesis in a transgenic mouse model of cerebral amyloidosis. *Neurosci Lett* 2004; **366**: 80–85.
30 Niwa K, Younkin L, Ebeling C, Turner SK, Westaway D, Younkin S *et al.* Abeta 1-40-related reduction in functional hyperemia in mouse neocortex during somatosensory activation. *Proc Natl Acad Sci USA* 2000; **97**: 9735–9740.

31 Wang H, Lynch JR, Song P, Yang HJ, Yates RB, Mace B *et al.* Simvastatin and atorvastatin improve behavioral outcome, reduce hippocampal degeneration, and improve cerebral blood flow after experimental traumatic brain injury. *Exp Neurol* 2007; **206**: 59–69.
32 Endres M, Laufs U, Huang Z, Nakamura T, Huang P, Moskowitz MA *et al.* Stroke protection by 3-hydroxy-3-methylglutaryl (HMG)-CoA reductase inhibitors mediated by endothelial nitric oxide synthase. *Proc Natl Acad Sci USA* 1998; **95**: 8880–8885.
33 Nagaoka T, Hein TW, Yoshida A, Kuo L. Simvastatin elicits dilation of isolated porcine retinal arterioles: role of nitric oxide and mevalonate-rho kinase pathways. *Invest Ophthalmol Vis Sci* 2007; **48**: 825–832.
34 Laufs U, Liao JK. Direct vascular effects of HMG-CoA reductase inhibitors. *Trends Cardiovasc Med* 2000; **10**: 143–148.
35 Wu H, Jiang H, Lu D, Qu C, Xiong Y, Zhou D *et al.* Induction of angiogenesis and modulation of vascular endothelial growth factor receptor-2 by simvastatin after traumatic brain injury. *Neurosurgery* 2011; **68**: 1363–1371.
36 Li B, Mahmood A, Lu D, Wu H, Xiong Y, Qu C *et al.* Simvastatin attenuates microglial cells and astrocyte activation and decreases interleukin-1beta level after traumatic brain injury. *Neurosurgery* 2009; **65**: 179–185.
37 Mannix RC, Whalen MJ. Traumatic brain injury, microglia, and Beta amyloid. *Int J Alzheimers Dis* 2012; **2012**: 608732.